EUROPEAN COMMISSION

Community Research

# RAPHAEL

**Contract Number: 516508 (FI6O)**

**DELIVERABLE (D-FT4.1)**

# ATLAS – statistical approach – sensitivity analysis


Author(s): **Gilles Pujol**
**Claire Cannaméla**


Reporting period: e.g. 15/04/2005– 14/04/2007

Date of issue of this report: 19/01/2006

Start date of project: **15/04/2005** Duration: **48 Months**


| Project co-funded by the European Commission under the Euratom Research and Training Programme on Nuclear Energy within the Sixth Framework Programme (2002-2006) | | |
|---|---|---|
| **Dissemination Level** | | |
| **PU** | Public | |
| **RE** | Restricted to the partners of the RAPHAEL project | |
| **CO** | Confidential, only for specific distribution list defined on this document | **X** |


**RAPHAEL** ***(ReActor for Process heat, Hydrogen And ELectricity generation)***

# Distribution list

| Person and organisation name and/or group | Comments |
|---|---|
| OBRY Patrick (CEA) | |
| PHÉLIP Mayeul (CEA) | |
| MICHEL Frédéric (CEA) | |
| PELLETIER Michel (CEA) | |
| HEYRAUD Phillippe (CEA) | |
| CANNAMÉLA Claire (CEA) | |
| PUJOL Gilles (CEA) | |
| WERNER Heinz (FZJ) | |
| NABIELEK Heinz (FZJ) | |
| OVER Hans Helmut (JRC/IE) | |
| ABRAM Tim (Nexia Solutions) | |
| MARTIN David (Nexia Solutions) | |
| GUILLERMIER Pierre (AREVA NP) | |
| SHIHAB Sammy (BN) | |
| TOURY Grégoire (BN) | |
| CHAUVET Vincent (STEP) | |
| BOGUSH Edgar (FANP GmbH) | |
| CASALTA Sylvie (EC) | |

| **ReActor for Process heat, Hydrogen And ELectricity generation (RAPHAEL)** | | |
|---|---|---|
| **Sub-project :** SP-FT<br>**Work package :** 4 | **RAPHAEL document no :**<br>RAPHAEL-0601-D-FT4.1 | **Document type :**<br>Deliverable |
| **Issued by :** CEA (FR)<br>**Internal no. :** NT DEC/SESC/LSC/06-003 | | **Document status :**<br>Final |

| **Document title** |
|---|
| **ATLAS – statistical approach – sensitivity analysis** |

## Abstract

The ATLAS computational code developed by the CEA is designed to simulate the behaviour of high temperature reactor fuel: coated particle fuel. This note will discuss a preliminary statistical study carried out using this computational code. The code parameters are not considered constant but variable in a certain range. This study aims at determining the parameters that entail variations responsible for fuel particle failure. Firstly, the theory behind sensitivity analyses will be explained, describing a complete range of methods: the linear index method (SRC, PCC, etc.), MORRIS method, SOBOL method and FAST method.

Next, studies carried out on the ATLAS code all bear three problems in mind: uncertainty related to statistical variations in fuel particles, uncertainty related to variations in reactor irradiation conditions and uncertainty related to material behaviour laws. The effects of these three sources of uncertainties upon stress responsible for particle failure are examined.

This research aims at demonstrating the utility of sensitivity studies. On the one hand, sensitivity studies can be helpful in modelling as they make it possible to better understand the phenomena involved. On the other hand, sensitivity studies provide valuable information required to carry out reliability studies.

**Revisions**

| Rev. | Date | Short description | Author | WP Leader | SP Leader | Coordinator |
|---|---|---|---|---|---|---|
| 00 | 05/04/2006 | First issue | G. PUJOL<br>CEA | P. OBRY<br>CEA | M. PHÉLIP<br>CEA | E. BOGUSCH<br>AREVA NP<br>GbmH |
| | | | | | | |
| | | | | | | |
| | | | | | | |

Direction de l'énergie nucléaire
Département d'études des combustibles
Service d'études et de simulation du comportement des combustibles

D
E
C

CADARACHE

# ATLAS - statistical approach - sensitivity analysis
# ATALS - approche statistique - analyse de sensibilité

G. Pujol, C.Cannaméla

Note Technique SESC/LSC 06-003 – Indice 0 – avril 2006

Commissariat à l'énergie atomique
Centre de Cadarache
DEN/CAD/DEC/SESC/LSC - Bât 151 - 13108 SAINT-PAUL-LEZ-DURANCE CEDEX
Tél. : 04.42.25.38.62- Fax : 04.42.25.29.49– Mail : sesclsc@drncad.cea.fr

Direction de l'énergie nucléaire
Département d'études des combustibles
Service d'études et de simulation du comportement des combustibles
Laboratoire de simulation de comportement du combustible

# ATLAS - STATISTICAL APPROACH - SENSITIVITY ANALYSIS
# ATALS - APPROCHE STATISTIQUE - ANALYSE DE SENSIBILITÉ

| | | | |
|---|---|---|---|
| **Auteur(s)** | **G. Pujol*, C. Cannamela** | | |
| **Référence note** | **Note Technique SESC/LSC 06-003 – Ind. 0** | | |
| Cadre de réalisation | DDIN/SFS/A-SCRCG | | |
| Classification | Libre | | |
| N° EOTP | A-SCRCG-05-01 | Nombre de pages : | 55 |

CEA/DEN/CAD/DEC/SESC
DO 99 05/04/06

* *Manpower*

Référence et date de la diffusion initiale :

06PPJP000130

**Résumé :**

Cette note présente une première analyse de sensibilité du code ATLAS. C'est une étude statistique. Les différentes sources d'incertitudes sont identifiées et caractérisées. Elles proviennent des variations statistiques des caractéristiques des particules, des variations des conditions d'irradiation, ainsi que des lois de comportement des matériaux. Nous étudions la répercussion de ces incertitudes sur la rupture des particules.

**Abstract :**

This note will discuss a preliminary sensitivity analysis of the ATLAS computational code. Methods rely on statistics. The different source of uncertainty are identified and characterized. They come from statistical variations in fuel particles properties, variations in reactor irradiation conditions, and material behaviour laws. The effects of these three sources of uncertainties upon particle failure are examined.

| | REDACTEUR | VERIFICATEUR | APPROBATEUR | ÉMETTEUR |
|---|---|---|---|---|
| NOM | G. PUJOL | F. MICHEL | P. OBRY | L. BRUNEL |
| VISA | | F. Michel | | |

AFAQ ISO 9001 VERSION 2000
DEC

# LISTE DE DIFFUSION

## DIFFUSION EXTERNE

| SOCIÉTÉ | NOM DU DESTINATAIRE | NOMBRE D'EXEMPLAIRES | OBSERVATIONS |
|---|---|---|---|
| FZJ | M. WERNER | R | R = RÉSUMÉ |
| | M. NABIELEK | R | DOCUMENT SUR SINTER |
| JRC/IE | M. OVER | R | |
| NEXIA SOLUTIONS | M. ABRAM | R | |
| | M. MARTIN | R | |
| AREVA NP | M. GUILLERMIER | R | |
| | M. MAILHE | R | |
| | MLLE DANIEL | R | |
| BN | M. SHIHAB | R | |
| | M. TOURY | R | |
| STEP | M. CHAUVET | R | |
| AREVA NP GMBH | M. BOGUSH | R | |
| EC | MME CASALTA | R | |

## DIFFUSION INTERNE

| Dpt/Service/Labo | NOM DU DESTINATAIRE | NOMBRE D'EXEMPLAIRES | OBSERVATIONS |
|---|---|---|---|
| DEN/DDIN/DPSF | M. ANZIEU | 1 | R = RÉSUMÉ |
| | M. MATHONIERE | R | DOCUMENT SUR INTRADEC |
| DEN/DSOE/SIM | M. CHAULIAC | R | |
| | M. BRUN | 1 | |
| DEN/DDIN/CCC | M. BROSSARD | R | |
| DM2S/SERMA/LCA | M. RAEPSAET | R | |
| DEC | | R | |
| DEC/SESC | | 1+R | |
| DEC/SESC/LLCC | | R | |
| DEC/SESC/LIPA | | R | |
| DEC/SESC/LC2I | | R | |
| | M. PHELIP | 1 | |
| | M. DEGENEVE | R | |
| DEC/SESC/LSC | M. OBRY | 1 | |
| | M. MICHEL | R | |
| | M. PELLETIER | 1 | |
| | MLLE CANNAMELA | 1 | |
| | M. HEYRAUD | R | |
| | M. PUJOL | 1 | |
| | TOUS | R PAR @ | |

# RÉVISIONS

| DATE | OBJET DES RÉVISIONS | INDICE |
|---|---|---|
| AVRIL 2006 | ÉMISSION INITIALE | 0 |

# TABLE OF CONTENTS

# 1. INTRODUCTION

France currently has a total of 58 second-generation reactors, all based on pressurised water reactor technology (PWR). Renewal of this nuclear park should begin around 2015 with the construction of third-generation reactors (EPR). These reactors will provide enhanced safety but are not suitable for developing countries with electric grids that cannot manage reactors with high unit power.

This observation opened the way to research into other reactor technologies, such as the high temperature reactor (HTR). This reactor has the following characteristics:

- Operates at high temperatures (above 1000°C in the VHTR concept), therefore enabling high efficiency; this characteristic also makes it possible to produce hydrogen as well as electricity;
- Produces low power density (2 to 7 $MW.m^{-3}$ in comparison with 100 $MW.m^{-3}$ for the current PWR reactors), permitting a unique level of safety.

These advantages are obtained thanks to the combination of three main specificities:

- Cooling by an inert gas such as helium;
- Use of large quantities of graphite as the moderator;
- Use of coated particle fuel that is particularly refractory and designed to retain fission products.

The HTR design is also considered as a step towards the future fourth-generation reactors.

Particle fuel comes in the shape of coated micro-beads less than a millimetre in diameter (cf. Figure 1(a)). Each particle is composed of a fuel kernel coated in different layers of refractory materials. In terms of the options currently available, the fuel kernel is composed of uranium oxide ($UO_2$) and coated in four ceramic layers (TRISO particles). From the kernel outwards, the following layers are found (cf. Figure 1(b)):

- A layer of porous carbon, known as the buffer, used as a reservoir to collect fission gases released by the kernel;
- A layer of dense pyrolitic carbon (PyC) contributing to the mechanical strength of the fuel particle;
- A layer of silicon carbide (SiC) guaranteeing the leaktightness of the particle vis-à-vis fission products;
- A layer of dense pyrolitic carbon (PyC) also guaranteeing the mechanical strength of the fuel particle.

This design boasts the following advantages:

- Excellent containment of fission products (leaktightness is ensured in the event of an accident up to 1600°C), therefore making it possible to reach high operating temperatures;

- Broad range of possibilities in terms of material combinations and geometrical & physical parameters. For example, the fuel kernel can be made of uranium oxide, thorium or a mixture of uranium and plutonium.

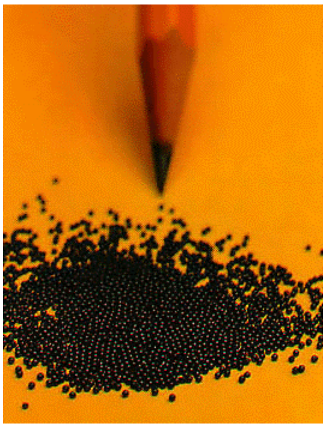

(a)

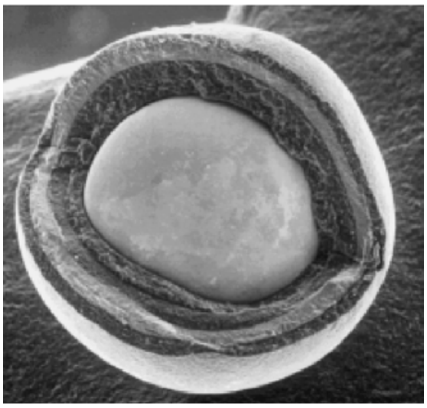

(b)

FIGURE 1 : COATED PARTICLE FUEL

The particles are not positioned freely within the kernel reactor but agglomerated in a graphite matrix to form manipulable cylindrical or spherical objects:

- *Fuel elements* (cf. Figure 2 (a)) are small cylinders with a diameter of 1 to 2 cm and a length of 5 to 6 cm. They are inserted inside large prismatic graphite blocks with a hexagonal cross-section (about 30 cm in diameter and 80 cm high). Channels are drilled in these blocks to permit the flow of the gas coolant;
- *Pebbles* (cf. Figure 2 (b)) are graphite spheres with a diameter of about 6 cm; the core is therefore composed of an unorganised stack of these particles, with the coolant circulating between the spaces created by such stack geometry.

A HTR core is therefore going to contain a considerable quantity of fuel particles (about $10^9$).

(a)

(b)

FIGURE 2 : FUEL ASSEMBLIES

The ATLAS computational code is developed by the CEA (DEC/SESC/LSC) with the aim of simulating the behaviour of this type of fuel under irradiation.
A specific problem that the LSC laboratory is investigating concerns the failure of these fuel particles (cf. Figure 3). This accidental situation results in the release of fission products into the primary system coolant. For the moment, ATLAS cannot determine the particle failure rate in a given configuration; this will require the integration of probabilistic models.

Within this framework, we intend to carry out a preliminary study on the behaviour of the ATLAS computational code in terms of input parameter uncertainties. This approach is known as a *sensitivity analysis* and relies on a series of statistical methods.

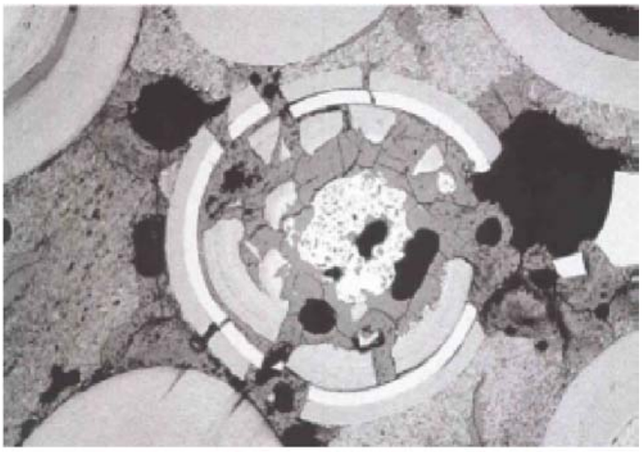

*Particle failure leads to the release of fission products.*

FIGURE 3 : PARTICLE FAILURE

# 2. BIBLIOGRAPHY OF SENSITIVITY ANALYSIS METHODS

The branch of sensitivity studies is rather new. Sensitivity studies have become more popular as computers have become increasingly more powerful. Following a period marked by methods drawn from differential calculation, current methods now rely on statistics. Andrea SALTELLI's team is very active in this field, with his publication [1] considered as the main reference in this bibliography.

## 2.1. OBJECT AND SCOPE

A sensitivity analysis is still not a very widespread approach. This subsection intends to demonstrate that a sensitivity analysis represents an important stage in modelling.

**Source of the problem**

A code is a computer programme that calculates results based on input parameters. A computational code is used for two different reasons:

- Prognostics (direct problem): calculating the code output corresponding to a given set of input parameters;
- Diagnostics (inverse problem): determining input parameters so that the output validates a property. For example, calibration aims at adjusting the code output to experimental data.

In both cases, *uncertainty* always exists when using a computational code. Uncertainty results from the assimilation of real data. Two types can be distinguished:

- The quantities are known with limited accuracy: such quantities may have been obtained experimentally (and not necessarily under representative conditions) or resulted from expert judgements;
- The quantities are subject to statistical variations: this type of uncertainty is encountered when the object under investigation belongs to a population.

Taking into account this uncertainty, it is thus possible to examine the problem of the computational code's reliability. In terms of prognostics, uncertainties on input data influence the output data. Therefore, even a code relying on very good modelling can produce mediocre results. In terms of diagnostics, research on the optimal combination of parameters no longer makes any sense. For example, in terms of calibration, experimental results measured with a certain margin of error tend to point to considering all acceptable values of parameters. The serious use of a computational code is therefore to be reconsidered in the light of uncertainty: this is our objective.

### Model and uncertainty

A *model* ensures the connection between input uncertainty and output uncertainty. The term "model" shall be referred to as a function that associates an output value or *response* with parameters called *factors*. Hence the following expression:

$$\begin{array}{cccc} f: & \Re^p & \to & \Re \\ & (x_1,\ldots,x_p) & \mapsto & y = f(x_1,\ldots,x_p) \end{array}$$

The model is not the computational code:

- A factor models a source of uncertainty on given data; it is not necessarily a code input parameter but a combination of parameters for example, a coded "hard" value, etc.,
- The response is a unique real value, whereas the code output data are often multiple and functional. The response is computed based on such output data and must be chosen to accurately represent the phenomenon under investigation. The fact that the response is unique is not restrictive: several analyses for several responses.

Uncertainty on factors is modelled by a probability distribution: the vector $(x_1,\ldots,x_p)$ is the result of a random vector $(X_1,\ldots,X_p)$. The response $y$ is therefore a result of the random variable $Y = f(X_1,\ldots,X_p)$. Therefore, uncertainty is an integral part of the model.

### Sensitivity

Model *sensitivity* can be described as the variation in the response in relation to variations in the factors. Sensitivity can be expressed by the following partial derivatives:

$$\frac{\partial Y}{\partial X_i} = \frac{\partial f}{\partial x_i}(X_1,\ldots,X_p)$$

The expression of the derivatives with the random variables indicates that the factors vary according to their probability distribution. A factor will vary more rapidly in a region where it is less likely to be found, and less rapidly in a region where it is more likely to found.

This notion is known as local sensitivity in literature. Historically speaking, this was the first attempt at defining the concept of sensitivity based on finite differences methods used to evaluate derivatives. The notion discussed here within differs slightly so as to take into account factor distributions. As seen previously, uncertainty is considered to be an integral part of the model.

**Influence**

The *influence* or effect of a factor upon the response is the fraction of the response's uncertainty caused by this factor. It is the combination of factor uncertainty and the model's sensitivity, with the latter acting as a coefficient of amplification. For example, high uncertainty on a factor associated with low sensitivity on the same factor will produce very little consequence. This notion is referred to as global sensitivity in literature, however we consider the term "influence" to be more appropriate.
Influence is usually expressed in terms of variance.

Thanks to McKay, an attempt at defining this notion was made: the quantity referred to as the *correlation ratio*

$$S_i = \frac{Var(E(Y/X_i))}{Var(Y)}$$

is an index of influence of the $i^e$ factor on the response:

- The greatest influence that $X_i$ can have upon $Y$ is modelled by $E(Y/X_i) = Y$, and therefore $S_i = 1$;
- The absence of influence of $X_i$ is expressed as the independence, that is, $E(Y/X_i) = E(Y)$, and therefore $S_i = 0$.

**Sensitivity analysis**

This expression regroups the analysis of uncertainty, sensitivity and influence. The most standard objectives behind such analyses are:

- *Prioritisation of factors*: classifying factors by order of importance; if a factor has influence by lack of information (and then over-estimated), it may be a good idea to improve knowledge of this factor (retrieval of information, measuring campaigns, etc.);
- *Reduction of the number of factors*: classifying the factors into two categories: influential parameters, non-influential parameters; the model can therefore be simplified in terms of the former, whereas the latter can be considered as constants;
- *Reduction of the variance*: obtaining a given improvement of the response by acting on the least possible number of factors;
- *Discriminant power*: determining all factors responsible for the presence of the response in a given region.

These objectives show that a sensitivity analysis offers a targeted approach, aiming at demonstrating a hypothesis.

A description of the sensitivity analysis methods is provided below.

## 2.2. LINEAR MODEL STUDY

This subsection focuses on a linear model of the following form:

$$Y = b_0 + \sum_{j=1}^{p} b_j X_j + \varepsilon$$

In practice, it is not known if this model is linear. Analysis is therefore performed based on a linear regression of the model, on the condition that this regression is considered reliable[1]. In the case where the linear regression is not correct, information on the indices can still be taken into account when considered qualitatively (classification of the factors by order of importance).

The method involves estimating different influence indices based on a sample of factors:

$$X = \begin{pmatrix} X_{11} & \dots & X_{1p} \\ \vdots & & \vdots \\ X_{n1} & \dots & X_{np} \end{pmatrix}$$

**Correlation coefficients (PEAR)**

The Pearson correlation coefficient between the factor $X_j$ and the response $Y$ is given by the expression:

$$PEAR_j = \frac{\sum_{i=1}^{n} (X_{ij} - E(X_j))(Y_i - E(Y))}{\left[\sum_{i=1}^{n} (X_{ij} - E(X_j))^2\right]^{1/2} \left[\sum_{i=1}^{n} (Y_i - E(Y))^2\right]^{1/2}}$$

This formula calculates the linear relationship between the variables $X_j$ and $Y$. This coefficient is equal to ±1 if and only if $Y = aX_j + b$, and if $X_j$ and $Y$ are independent then the coefficient is equal to zero (the reciprocal is generally erroneous). A positive sign indicates that the variables are progressing in the same direction, whereas a negative sign indicates the opposite direction.

[1] See [2] on the theory of linear regression.

**Standardised regression coefficients (SRC)**

The standardised regression coefficient corresponding to the factor $X_j$ is defined as follows:

$$SRC_j = \frac{Var(X_j)}{Var(Y)} b_j^{\,2}$$

The SRC indices are the square roots of the linear regression model coefficients, with the factors and response of this model having been standardised. These coefficients therefore calculate the effect of an input variable on the output variable. If the input variables are independent, their sum is equivalent to 1; they therefore represent the variance decomposition of the response. In this case, a standardised regression coefficient will compute the fraction of the response variance due to a factor.

The linear regression theory guarantees that the SRCs are square roots of the Pearson coefficients (cf. [2]). However, we shall retain both classes of indices. Pearson's indices provide information on the sign, thus the direction of the influence, whereas the SRCs quantify the influence by variance decomposition.

**Partial correlation coefficients (PCC)**

When factors are correlated, SRCs are much less relevant. For example, in the case of three variables correlated two by two $X_1$, $X_2$ and $Y$, it is not possible to determine the influence of $X_1$ only upon $Y$ as the effects of $X_2$ are implicit. Partial correlation coefficients are introduced to solve this problem and are expressed as such:

$$PCC_j = Cor(Y - \hat{Y}, X_j - \hat{X}_j)$$

where:

- $\hat{Y}$ represents the prediction of the linear model in which $X_j$ is not present, this model is expressed as:

$$Y = c_0 + \sum_{k \neq j} c_k X_k + \varepsilon_1$$

- $\hat{X}_j$ represents the prediction of the linear model expressing $X_j$ in relation to the other factors, this model is expressed as:

$$X_j = d_0 + \sum_{k \neq j} d_k X_k + \varepsilon_2$$

PCCs compute the linear correlation between a response and a factor after having carried out a correlation designed to neutralise the (linear) correlations between the input data. They range between -1 and 1 and can be interpreted as correlation coefficients. Strictly speaking, this is not a measurement of influence but more so of linearity. Interpretation is complicated and it is better to consider this measurement in qualitative terms.

**Rank analysis**

When the relationship between $Y$ and the $X_j$ is not linear but monotonic, the preceding analysis can therefore be performed in terms of ranks. Instead of considering the values of $Y$ and $X_j$ products, their ranks are calculated: 1 for the smallest value, etc. and *n* for the biggest value (cf. table 1). A monotonic relationship in relation to each factor can be expressed by a linear relationship based on the ranks. The same indices are therefore calculated, only the names change:

- Pearson coefficients become Spearman coefficients;
- SRCs become standardised rank regression coefficients (SRRC);
- PCCs become partial rank correlation coefficients (PRCC).

Interpretation is more complicated as the model is no longer studied directly. Information is therefore to be considered in qualitative terms.

| Y | X1 | X2 | X3 | X4 | RANK(Y) | RANK(X1) | RANK(X2) | RANK(X3) | RANK(X4) |
|---|---|---|---|---|---|---|---|---|---|
| -0.21 | -1.91 | 0.56 | 0.14 | -0.27 | 3 | 1 | 3 | 3 | 2 |
| -1.01 | 0.57 | 0.91 | -1.54 | -0.38 | 1 | 3 | 4 | 1 | 1 |
| 0.65 | 0.34 | -0.90 | 0.10 | 0.87 | 4 | 2 | 2 | 2 | 4 |
| -0.71 | 0.76 | -1.37 | 0.81 | -0.16 | 2 | 4 | 1 | 4 | 3 |

TABLE 1 : EXAMPLE OF RANK TRANSFORMATION

## 2.3. MORRIS SCREENING METHOD

Experience shows that in the case of a model with many factors, only a few factors are influential. Screening methods aim at rapidly defining these factors. These methods rely on experiment designs and provide qualitative information, that is to say, they make it possible to classify the factors by order of importance without quantification. Screening analyses provides valuable data at lower costs. They are often used to “prune” a model that is complex or costly in terms of runtime before being used to study this model using better methods.

The MORRIS method makes it possible to classify factors into three categories:

1. Factors with negligible effects,
2. Factors with linear effects without interactions,
3. Factors with non-linear effects and/or interactions.

**Elementary effects**

It is assumed that all factors follow a uniform distribution $U(0,1)$. The space of the factors $[0,1]^p$ is discretised according to a p-dimensional grid:

$$\left\{0,\frac{1}{n-1},\frac{2}{n-1},\ldots,\frac{n-2}{n-1},1\right\}^p$$

Let $\Delta$ be a positive multiple of $\frac{1}{n-1}$. The elementary effect i[e] is the variation of the model disturbed in the direction i[e], or:

$$d_i=\frac{y(x+\Delta e_i)-y(x)}{\Delta}$$

where $e_i$ is the canonical base vector i[e]. Of course, the point $x$ must be such that $x+\Delta e_i$ remains within $[0,1]^p$.

**Sensitivity measurements**

It is possible to define sensitivity measurements based on elementary effects:

$$\mu_i^*=E(|d_i|)$$
$$\sigma_i=\sigma(d_i)$$

These measurements are in fact sensitivity measurements but are averaged over the whole range instead of being measured locally.

Interpretation of these quantities is rather simple:

- $\mu_i^*$ is a measurement of the model sensitivity for the factor i[e]; if $\mu_i^*$ is very low, then the elementary effects are insignificant; however, if $\mu_i^*$ is high, then the elementary effects are generally significant;
- $\sigma_i$ is a measurement of the non-linearity or the interactions (without being able to distinguish between the two); if $\sigma_i$ is low, the elementary effects are identical: they are linear and without interactions (seeing that the effects are similar, they do not depend on the position in space, thus on the value of other factors); on the contrary, if $\sigma_i$ is high, then the elementary effects are notably different from each other: they are non-linear, with interactions or both.

A graph $(\mu^*, \sigma)$ is used to easily distinguish between the different groups.

**Experiment design**

When the number of factors is high, the elementary effects can only be calculated for a reduced number of points as the number of calls on the model must remain reasonable. All combinations of factors required for analysis constitute a factorial experiment design.

The MORRIS experiment design has two remarkable characteristics:

- Two successive simulations only differ by one factor; this characteristic is called "One At a Time (OAT);
- The experiment design is random.

The matrix points of the experiment design form a *random walk* in $[0,1]^p$ (several examples are provided in Figure 4). It is a matrix ($p$+1)*$p$ such that:

- Two consecutive lines are identical except for a value where they differ by ±Δ (OAT characteristic);
- This occurs once only for each coordinate,

and can be formally expressed as:

$$B^* = (x_j^i)_{\substack{i=1\ldots p+1 \\ j=1\ldots p}}$$

with:

$$\begin{cases} \forall i, \exists! j_i, x^{i+1} = x^i + \Delta e_{j_i} \\ j_i = j_{i'} \Rightarrow i = i' \end{cases}$$

The elementary effects are therefore expressed as:

$$d_{j_i}(x^i) = \pm \frac{y(x^{i+1}) - y(x^i)}{\Delta}$$

The matrix of the experiment design $B$* can be represented by the following expression:

$$B^* = \left( J_{p+1,1}.x^* + \frac{\Delta}{2}\left((2B - J_{p+1,p})D^* + J_{p+1,p}\right)\right)P^*$$

with:

- $J_{i,j}$ = $i$ *$j$ matrix filled with ones;
- $B$ = ($p$+1)*p matrix with ones in the lower triangular part and zeros in the upper part;
- $D^*$ = $p$*$p$ diagonal matrix composed of equiprobable + ones and – ones;
- $P^*$ = $p$*$p$ random permutation matrix;
- $x^*$ = randomly chosen point on the grid;

on the condition that the points of the experiment design (matrix lines) remain on the grid. A method used to guarantee this involves repeating the sampling of the point $x^*$ until evidence of the contrary.

The lines *i* and *i*+1 of the $B^*$ matrix are used to calculate the elementary effect $f_j^e$, with *j* being such that $P^*(i,j)=1$. The sign of this effect (did we add or subtract $\Delta$?) is $D^*(i,i)$. By expressing $y=f(B^*)$, the vector of the elementary effects $d$ (effect per factor) is therefore expressed by[2]:

$$d=\left(\frac{(y_2,\ldots,y_{p+1})-(y_1,\ldots,y_p)}{\Delta}\right).D^*.P^*$$

By constructing *r* experiment designs, it is possible to obtain *r* $d$ vectors. These vectors obtain *r* elementary effects for each factor, that is, an *r*-sample of the $d_i$ distribution for each *i*. The statistics $\mu_i^*$ and $\sigma_i$ are easy to estimate based on this sample by using standard mean and standard deviation estimators.

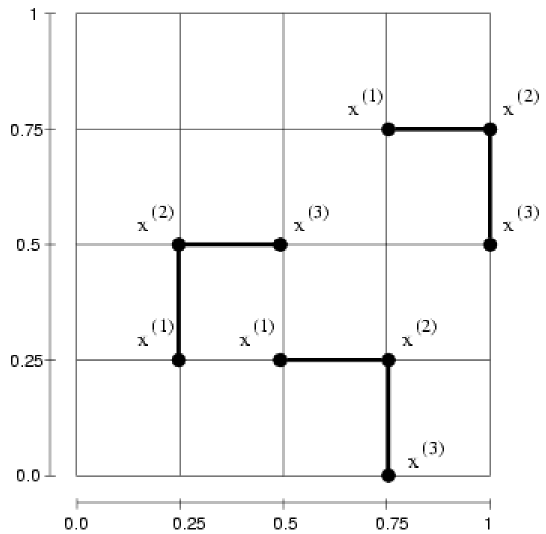


*The experiment design relies on the discretization of space (two factors in this case). Three possible paths are represented. The three points of each path represent the values of the experiment design (matrix lines). They make it possible to evaluate two elementary effects, one for each direction.*

FIGURE 4 : MORRIS EXPERIMENT DESIGN

[2] This formula – overlooked in current literature – is only useful for implementation.

**Choice of parameters**

The choice of *n*, Δ and *r* parameters is very important. SALTELLI (according to MORRIS) recommends Δ = *n*/(2(*n* – 1)) with even *n*. We prefer a low Δ value (of about 1/(*n* – 1)) with a rather big *n*. The elementary effects therefore represent more local variations. However, the number of *r* repetitions required to sufficiently explore the space is higher. The choice of Δ and *n* depends on the number of simulations that we want to perform (this number is equal to (*p*+1)**r*).

## 2.4. SOBOL METHOD

The SOBOL method is the most general method used to analyse influence and relies on variance decomposition. Four families of indices are available:

- First order indices expressing the influence of one factor only;
- Indices of greater order expressing the influence of interactions between several factors;
- Total indices expressing the total influence of a factor, including interactions;
- Multi-dimensional indices enabling the preceding analyses in the case where the factors are correlated.

**SOBOL indices**

For an integratable function $f$ on $[0,1]^p$, the following unique decomposition was computed:

$$Y = f(X_1,\ldots,X_p) = f_0 + \sum_{1\le i\le p} f_i(X_i) + \sum_{1\le i<j\le p} f_{ij}(X_i,X_j) + \ldots + f_{12\ldots p}(X_1,\ldots,X_p)$$

where $f_0$ is a constant and:

$$\int_0^1 f_{i_1\ldots i_s}(x_{i_1},\ldots,x_{i_s})dx_{i_k} = 0, \forall\{i_1,\ldots,i_s\} \subseteq \{1,\ldots,p\}, \forall k = 1,\ldots,s$$

The variance can also be broken down into sums:

$$Var(Y) = \sum_{i=1}^{p} V_i + \sum_{1\le i<j\le p} V_{ij} + \sum_{1\le i<j<k\le p} V_{ijk} + \ldots$$

with:

$$V_i = Var(E(Y/X_i))$$
$$V_{ij} = Var(E(Y/X_i,X_j)) - V_i - V_j$$
$$V_{ijk} = Var(E(Y/X_i,X_j,X_k)) - V_{ij} - V_{ik} - V_{jk} - V_i - V_j - V_k$$
$$\ldots$$

If the factors $X_i$ are independent, then:

$$V_{i_1 i_2 \ldots i_s} = Var(f_{i_1 i_2 \ldots i_s}(X_{i_1}, X_{i_2}, \ldots, X_{i_s}))$$

and the indices of influence are expressed as:

$$S_{i_1 i_2 \ldots i_s} = \frac{V_{i_1 i_2 \ldots i_s}}{Var(Y)}$$

The first order indices of influence are identical to the MCKAY indices discussed in subsection 2.1. They convey the fraction of the variance of the response owing to one single input variable. The second order indices of influence express the fraction of the variance of owing to the interaction of two input variables (not taken into account by the single variables), and so forth for the greater orders. The number of these indices increases factorially with the number of factors and, in practice, it is already difficult to estimate all indices up to the second order.

**Total indices**

The total influence indices express the fraction of the variance of the response owing to all contributions of a factor. To do this, all indices related to a factor are totalled, that is:

$$S_i^{tot} = \sum_{K\#i} S_K$$

In practice, indices of all orders are not required for computations. Total indices compute estimates as easily as first order indices. Total indices are therefore very useful as they provide comprehensive information on a factor at a lower cost.

**Multi-dimensional indices**

The PhD thesis by Julien JACQUES [3] reveals that the preceding indices are no longer relevant in the case of correlated factors. He recommends regrouping the correlated variables between themselves and calculating the indices between the correlation groups. More specifically, new variables are introduced (after renumbering):

$$\widetilde{X}_1 = (X_1, \ldots, X_{n1})$$
$$\widetilde{X}_2 = (X_{n1+1}, \ldots, X_{n2})$$
$$\ldots$$

with independent $\widetilde{X}_i$ two by two. This brings us back to the case of independent factors with the indices that we just discussed.

Therefore, the first order index of the couple of correlated variables $(X_i, X_j)$ is expressed as:

$$S_{\{i,j\}} = \frac{V_{\{i,j\}}}{Var(Y)}$$

where:

$$V_{\{i,j\}} = Var(E(Y/X_i, X_j))$$

**Estimation**

To estimate $V_i$, the quantity $Var(E(Y/X_i))$ [3] is expressed as such:

$$\begin{aligned} Var(E(Y/X_i)) &= E(E(Y/X_i)^2) - E(E(Y/X_i))^2 \\ &= E(E(Y/X_i)^2) - E(Y)^2 \end{aligned}$$

The first term gives:

$$\begin{aligned} E(E(Y/X_i)^2) &= \int\left(\int f(x_1,\ldots,x_p)\prod_{j\neq i} dX_j\right)^2 dX_i \\ &= \int f(x_1^{(1)},\ldots,x_p^{(1)}) f(x_1^{(2)},\ldots,x_i^{(1)},\ldots,x_p^{(2)}) \prod_{i=1\ldots n} dX_i^{(1)} \prod_{j\neq i} dX_j^{(2)} \end{aligned}$$

This last integral is estimated by the sum:

$$E(E(Y/X_i)^2) \approx \frac{1}{n}\sum_{k=1}^{n} f(x_{k1}^{(1)},\ldots,x_{kp}^{(1)}) f(x_{k1}^{(2)},\ldots,x_{ki}^{(1)},\ldots,x_{kp}^{(2)})$$

which requires two independent computations of the *n*-sample:

$$x^{(1)} = \begin{pmatrix} \mathrm{x}_{11}^{(1)} & \cdots & \mathrm{x}_{1p}^{(1)} \\ \vdots & & \vdots \\ \mathrm{x}_{n1}^{(1)} & \cdots & \mathrm{x}_{np}^{(1)} \end{pmatrix} \qquad x^{(2)} = \begin{pmatrix} \mathrm{x}_{11}^{(2)} & \cdots & \mathrm{x}_{1p}^{(2)} \\ \vdots & & \vdots \\ \mathrm{x}_{n1}^{(2)} & \cdots & \mathrm{x}_{np}^{(2)} \end{pmatrix}$$

The estimator of $S_i$ is therefore:

$$\hat{S}_i = \frac{\hat{V}_i}{V\hat{a}r(Y)}$$

where:

$$\hat{V}_i = \frac{1}{n}\sum_{k=1}^{n} f(x_{k1}^{(1)},\ldots,x_{kp}^{(1)}) f(x_{k1}^{(2)},\ldots,x_{ki}^{(1)},\ldots,x_{kp}^{(2)}) - \hat{E}(Y)^2$$

[3] Sometimes written as variance of the conditional expectation (VCE).

The other indices compute in a similar manner (without justification) by:

$$\hat{S}_{ij} = \frac{\hat{V}_{ij}}{V\hat{a}r(Y)}, \ldots, \hat{S}_i^{tot} = 1 - \frac{\hat{V}_{\sim i}}{V\hat{a}r(Y)}, \ldots, \hat{S}_{\{i,j\}} = \frac{\hat{V}_{\{i,j\}}}{V\hat{a}r(Y)}, \ldots,$$

where:

$$\hat{V}_{ij} = \frac{1}{n}\sum_{k=1}^{n} f(x_{k1}{}^{(1)},\ldots,x_{kp}{}^{(1)}) f(x_{k1}{}^{(2)},\ldots,x_{ki}{}^{(1)},\ldots,x_{kj}{}^{(1)},\ldots,x_{kp}{}^{(2)}) - \hat{E}(Y)^2 - \hat{V}_i - \hat{V}_j$$

$$\ldots$$

$$\hat{V}_{\sim i} = \frac{1}{n}\sum_{k=1}^{n} f(x_{k1}{}^{(1)},\ldots,x_{kp}{}^{(1)}) f(x_{k1}{}^{(1)},\ldots,x_{ki}{}^{(2)},\ldots,x_{kp}{}^{(1)}) - \hat{E}(Y)^2$$

$$\hat{V}_{\{i,j\}} = \frac{1}{n}\sum_{k=1}^{n} f(x_{k1}{}^{(1)},\ldots,x_{kp}{}^{(1)}) f(x_{k1}{}^{(2)},\ldots,x_{ki}{}^{(1)},\ldots,x_{kj}{}^{(1)},\ldots,x_{kp}{}^{(2)}) - \hat{E}(Y)^2$$

$$\ldots$$

Two realisations of the *n*-sample are required to estimate an index, that is, 2*n* simulations. The same samples can be used to estimate the indices of all orders, but column substitutions entail new simulations. Therefore, a total of (*p*+1)**n* simulations is required to estimate the first order or total indices. In practice, *n* can easily be worth 10,000. This method is therefore suitable for analytical functions and response surfaces[4] rather than computational codes.

## 2.5. FAST METHOD

The Fourier Amplitude Sensitivity Test (FAST) method is based on a very simple notion: by making the factors oscillate – according to their own frequency – the response also varies according to the frequencies of the influential factors. This method was discovered by CUKIER in 1973 and recently improved by SALTELLI [4].

**Space transformations**

It is assumed that the factors obey uniform distributions $U(0,1)$. These factors are expressed by the following transformations:

$$X_i(S) = g_i(\sin(\omega_i S)), \quad S \sim U(-\pi,\pi)$$

[4] A response surface is a model designed to approximate a scatterplot as closely as possible. A technique used in sensitivity analyses consists in simulating a computational code for a reduced number of points, before constructing a response surface on which analyses will be performed.

where $\omega_i$ represent frequencies. These transformations imply that the factors will not obey uniform distributions and will not be independent. The choice of the functions $g_i$ and frequencies $\omega_i$ are necessary for maximum accuracy. A transformation that guarantees uniformity rather well is:

$$X_i(s) = \frac{1}{2} + \frac{1}{\pi}\arcsin(\sin(\omega_i s))$$

The frequency choices make it possible to ensure that all points in space $[0,1]^p$ are reached, which provides independence. This choice is detailed in the following paragraphs.

**Fourier decomposition**

When frequencies are both integer and positive, the following relationship applies:

$$E(Y) = \int_{[0,1]^p} f(x_1,\ldots,x_p)d(x_1,\ldots,x_p) = \frac{1}{2\pi}\int_{[-\pi,\pi]} f(x_1(s),\ldots,x_p(s))ds$$

Changing the variables therefore makes it possible to replace a multi-dimensional integral by a simple integral.

In terms of variance, the same change in variables was applied, thus producing the following expression:

$$\begin{aligned} Var(Y) &= \frac{1}{2\pi}\int_{[-\pi,\pi]} f^2(x_1(s),\ldots,x_p(s))ds - E(Y)^2 \\ &\approx \sum_{j=-\infty}^{+\infty}(A_j^2 + B_j^2) - (A_0^2 + B_0^2) \\ &= 2\sum_{j=1}^{+\infty}(A_j^2 + B_j^2) \qquad (2) \end{aligned}$$

where $A_j$ and $B_j$ represent the Fourier coefficients given by:

$$A_j = \frac{1}{2\pi}\int_{[-\pi,\pi]} f(x_1(s),\ldots,x_p(s))\cos(js)ds$$

$$B_j = \frac{1}{2\pi}\int_{[-\pi,\pi]} f(x_1(s),\ldots,x_p(s))\sin(js)ds$$

**First order indices**

The quantity $Var(E(Y/X_i))$ can be estimated by adding the terms in formula (2) only corresponding to the harmonic components of the $i^e$ frequency, written as follows:

$$V_i = 2\sum_{j=1}^{+\infty}({A_{j\omega_i}}^2 + {B_{j\omega_i}}^2)$$

and the first order index:

$$S_i = \frac{V_i}{V}$$

is the same as that found in the SOBOL method.

**Total indices**

SALTELLI recommends calculating the total-order sensitivity indices (extended FAST method) given by:

$$S_i^{tot} = 1 - \frac{V_{\sim i}}{V}$$

where $V_{\sim i}$ represents the sum of the harmonics of all frequencies other than i[e].

The term $V_{\sim i}$ is therefore equivalent to:

$$V_{\sim i} = \sum_{j \neq i} V_j$$

These are the same indices as the SOBOL total indices.

**Numerical aspect**

- The quantities $A_j$ and $B_j$ are computed by Monte-Carlo integration. Let $(s_1, \ldots, s_n)$ be a n-sample of the distribution $U(-\pi, \pi)$, then:

$$A_j \approx \frac{1}{2\pi}\sum_{i=1}^{n} f(x_1(s_i), \ldots, x_p(s_i))\cos(js_i)$$
$$B_j \approx \frac{1}{2\pi}\sum_{i=1}^{n} f(x_1(s_i), \ldots, x_p(s_i))\sin(js_i)$$

- The sums in the variance estimates are calculated up to a rank *M*. In practice, *M* = 4 is sufficient;
- The frequencies $\omega_i$ depend on the estimated index. The factor corresponding to the calculated index is attributed the highest frequency $\omega_{\max} = (n-1)/(2M)$. The other factors are attributed low frequencies that are uniformly distributed over $\{1, \ldots, \omega_{\max}/(2M)\}$.

<u>Comment</u>: once the quantities $A_j$ and $B_j$ have been estimated by the Monte-Carlo method, the indices – whether first-order or total-order – are computed by adding up the different harmonic components. Therefore, the same set of simulations is used to estimate a first-order index and a total-order index (seeing that the set of frequencies is the same for these two indices). This is an advantage

in comparison to the SOBOL method where *n* additional simulations were required to estimate the total indices.

## 2.6. CONCLUSION: IN PRACTICE

The approach applied when performing a sensitivity analysis is as follows:

1. Modelling uncertainty:
   - Determining the response so that it correctly indicates the phenomenon to be investigated; for example, if the computational code output is a function of time, a possible response is the value at the end time;
   - Determining the factors: listing all sources of uncertainty. Starting from the list of the computational code parameters is a good idea but it must be remembered that uncertainty does not necessarily concern the parameters as they appear; for example, if the computational code parameters are point coordinates, uncertainty may concerns the distance between these points;
   - Determining a probability distribution for each factor; all available sources of information are called upon to do this: literature, estimates on experimental data, expert judgements, etc.
   - Determining a correlation structure between the factors[5].

2. Uncertainty analysis: generating a sample, calculating the corresponding response and estimating certain characteristics of the response distribution (normality, moments, etc.); if the response varies very little, it is not necessary to continue;

3. Sensitivity analysis: choosing an analysis method in relation to objectives, generating an experiment design corresponding to this method, calculating the corresponding response and estimating the sensitivity indices.

Four sensitivity analysis methods have been discussed in this bibliography:

1. *Linear indices* (PEAR, SRC, PCC): this method is used to quantify the influence of each factor. This method has the advantage of being simple and effective while its disadvantage lies in the fact that it can only be applied if the linear regression is valid, which limits its range of application; adaptation to certain monotonic cases with rank transformation does extend this method's possibilities; it must be said that this method does not require any specific experiment design, which makes it possible to

[5] The correlation model is greatly dependent on the sample type (i.e. : rank correlation for a LHS sample) and therefore on the analysis method. It is therefore necessary to have an idea of the methods that will be applied. The approach is therefore not as linear as we would like it to be.

apply it to the sample used for the uncertainty analysis; this method is therefore worth testing before trying a more complex methods;

2. *MORRIS method*: this method is used to classify factors in order of influence, determine non-influential factors and identify those with non-linear effects or implied in interactions (without distinction in both cases); this method is very useful when the model has many factors as it requires very few simulations; we find this method has no disadvantages and recommend it prior to any in-depth study;

3. *SOBOL method*: this method is used to quantify the influence of each factor (single and total influence) and the interactions of all orders; this method can also take into account a correlation model with multi-dimensional indices; this is the most comprehensive method but has the disadvantage of demonstrating considerable variability in estimates: as many as 10 000 simulations per factor can be necessary to obtain correct estimates; we recommend using this method on a response surface; the latter can be constructed from the uncertainty analysis sample;

4. *FAST method*: this method is used to estimate the same indices as those for the SOBOL method but requires fewer simulations, which makes it a very interesting method.

All these methods should make it possible to carry out most sensitivity analyses. For any reader interested in other methods, we recommend work by SALTELLI [1] (particularly chapter 2 – Hitchhiker's guide to Sensitivity Analysis) and [4].

# 3. MODELLING ATLAS CODE UNCERTAINTY

The ATLAS code has not yet been subject to an uncertainty analysis. This preliminary study therefore aims at exposing the input sources of uncertainty (modelling stage) and describing the general behaviour of the code subject to this uncertainty (uncertainty, sensitivity and influence analyses).

Firstly, it is important to review the notions introduced in subsection 2.1. The model is an overlay of the computational code designed to model uncertainty under investigation. Factors are uncertain quantities that we vary and based on which the code input parameters are calculated. The response is calculated based on code outputs and must reflect the phenomenon under investigation.

It is also important to remember that particle failure (see section 1) is the phenomenon we are studying. Responses must therefore be significant indices of particle failure.
Before studying the uncertainties of these responses, the computing configuration used will be described.

## 3.1. COMPUTING CONFIGURATION

**Geometry**

The ATLAS application simulates the behaviour of coated particle fuel under irradiation (cf. section 1 for the fuel description, cf. [5] and [6] for a detailed description of the ATLAS code). This application resolves thermal and mechanical problems, as well as fission product diffusion by the finite-element method. For the time being, these problems are considered on a fuel particle scale. The geometry is therefore that of a particle. The computation range is an angular sector called 1D geometry and represented in Figure 5.

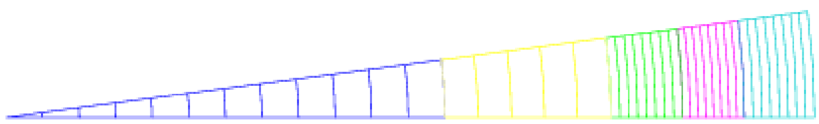

*The mesh corresponds to a TRISO particle, composed of – from the centre outwards – a fuel kernel, pyrolitic carbon buffer, a layer of dense pyrolitic carbon (IPyC), a layer of silicon carbide (SiC) and another layer of dense pyrolitic carbon (OPyC).*

FIGURE 5 : ATLAS COMPUTATION RANGE – 1D GEOMETRY

**Computation time**

The current version of the code is version 2.0. The improvements made in relation to version 1.0 involve 1) the porting of the application onto the PLEIADES platform and 2) resolving the diffusion problem. The addition of diffusion has no incidence on the section describing the mechanical behaviour, which is the only section that interests us. Furthermore, the more complex software architecture such as PLEIADES implies, for the time being, longer computation times (ATLAS version 1.0 is only a script of CAST3M[6] and operates about 4 times faster than version 2.0). The sensitivity studies that we carried out required several thousand simulations, equivalent to several days of computation. We therefore decided to use version 1.0. However, the results can be generalised to cover version 2.0, given the fact that the two versions do not differ for the problem under consideration.

**Irradiation history**

The irradiation history is an ATLAS code input. This set of parameters describes the external loads to which the particle is subjected. An irradiation history is composed of temporal variations of four different quantities:

- Temperature on the outer side of the particle;
- Pressure exerted by the coolant on the outer side of the particle;
- The fast fluence;
- Fission rate.

Figure 6 represents the temperature and fluence histories applied in our study. The irradiation history takes into account the entire life-cycle of the particles in a simplified manner, from manufacture to final burnup. The fission rate is considered proportional to the fast fluence. The external pressure is assumed constant over time.

[6] CEA finite-element code.

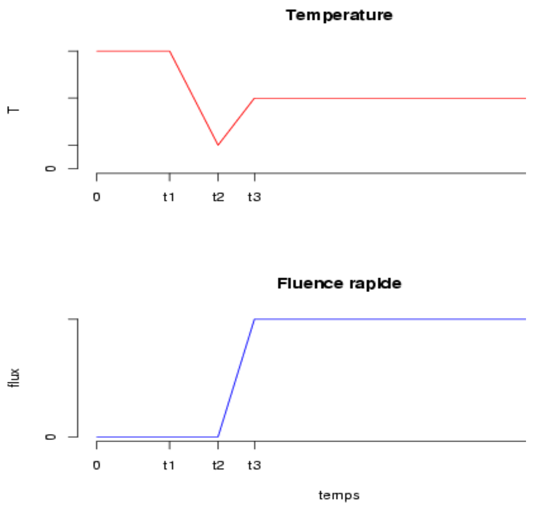


| Time interval | Description |
|---|---|
| [0, t1] *(6 days)* | Particle manufacturing |
| [t1, t2] *(1 day)* | Cooling to ambient temperature |
| [t2, t3] (5 minutes) | Reactor power build-up |
| [t3, t4] (up 15% FIMA) | Reactor operation |

FIGURE 6 : IRRADIATION HISTORY APPLIED IN CALCULATIONS

**Reactor**

The irradiation history characterises the reactor. It was decided to study two reactor configurations:

1. HFR-EU2: the high-flux reactor (HFR) is an experimental reactor located in Petten in the Netherlands. EU2 is the experiment's name.
2. GT-MHR: this gas turbine modular helium reactor (GT-MHR) is a production reactor project launched by the US (General Atomic) and Russia. Other partners have since joined them, including Framatome.

The GT-MHR was chosen for industrial applications of the ATLAS code. The experimental situation of the HFR was chosen so as to include our study in the existing research programme making it possible to validate the ATLAS code.

Furthermore, the EU2 experiment[7] will be used as a reference for the GT-MHR seeing that a compact-type fuel element is used in both cases. Table 2 provides data collected on the irradiation conditions in both reactors.

The framework within which calculations will be performed has now been established. The code input sources of uncertainty now remain to be identified. This is known as the modelling phase.

[7] Unfortunately, during our study, we learnt that the EU2 experiment is to be abandoned.

| | HFR-EU2 | | GT-MHR | |
|---|---|---|---|---|
| coolant pressure (bar) | 4.5 | (a) | 70 | (c) |
| min. temperature (K) | 1323 | (b) | 775 | (d) |
| max. temperature (K) | 1423 | (b) | 1175 | (d) |
| max. burn-up (%FIMA) | 10 | (b) | 13.7 | (e) |
| max. fast neutron flux (n.m-2) | 4.5e25 | (b) | 3.5e25 | (e) |
| irradiation time (EFPD) | 350 | (b) | 490 | (e) |
| nominal neutron flux (n.m-2.s-1) | 1.48e18 | | 8.28e17 | |
| nominal fission rate (s-1) | 3.30e-9 | | 3.23e-9 | |

*Source of data : (a) : [7], (b) : [8], (c) : [9], (d) : [10], (e) : [11]. The nominal neutron flux and nominal fission rate are calculated based on such data.*

TABLE 2 : IRRADIATION PARAMETER DATA

## 3.2. OUTPUT UNCERTAINTY

The mechanical failure of a particle can be caused by the failure of one of the dense outer layers (IPyC, SiC, OPyC). The most natural cause is too much strain in the SiC layer, though the PyC layers can also fail owing to stress generated by their densification, thus damaging the particle [12].

The responses we intend to study are the maximum tangential stresses in these layers (cf. Table 3). These maximum values are located:

- In space, on the inner sides of each layer;
- In time, near the beginning of irradiation for the PyC layers;
- In time, at the end of irradiation for the SiC layer in the case where the latter fails (the SiC layer rapidly undergoes compression during which it does not risk fracturing, before stress begins increasing regularly; the final value is therefore more representative of the maximum tension value capable of being reached).

The three responses are relevant indicators of particle failure.

Our research involves studying the uncertainty of these responses. To do this, it is necessary to take into account computational code input uncertainty.

| VARIABLE | DESCRIPTION |
| --- | --- |
| IPYC.SIGT.MAX | Maximum tangential stress on the inner side of the inner PyC layer |
| SIC.SIGT.FIN | Tangential stress at the end of irradiation on the inner side of the SiC layer |
| OPYC.SIGT.MAX | Maximum tangential stress on the inner side of the outer PyC layer |

TABLE 3 : STUDIED RESPONSES

## 3.3. INPUT UNCERTAINTY

The sources of uncertainty have been classified into three main categories:

1. *Particle manufacturing parameters*: variations in the particle characteristics are of a statistical nature (particles form a population) and depend on the manufacturing processes; these variations are rather well-known from manufacturing specifications and quality controls performed throughout the manufacturing process;
2. *Irradiation parameters*: particles are distributed in a random manner[8] in the reactor core; the external conditions to which these particles are subjected are variable and depend on their position and reactor design; the distributions of these quantities can be determined by neutronic and thermohydraulic calculations;
3. *Behaviour laws*: The physical properties and behaviour laws of materials are more or less well-known; uncertainty on these laws is often difficult to deal with in practice and mainly relies on expert judgements.

These three categories of uncertainty result in three series of factors: particle factors (PART, cf. Table 4), reactor factors (REAC, cf. Table 5) and law factors (LAWS, cf. Table 6).

One point must be specified in terms of the reactor parameters: two ATLAS irradiation parameters are the nominal neutron flux (FNN) and the nominal fission rate (PFN). These two parameters are related and their ratio – known as the acceleration factor (ACC) – is characteristic of a reactor type. It is therefore preferable to study the effect of this acceleration factor. The change in the variables, expressed below, makes it possible to consider the ACC and PFN factors as independent:

$$(FNN, PFN) \rightarrow (ACC = \frac{FNN}{PFN}, PFN)$$

[8] The term *random* is to be understood in a probabilistic sense: one particle has a certain probability to be found in each volume fraction of the reactor core. This distribution can be determined based on both the data on particle distribution in the fuel elements and the layout of these elements in the reactor core.

This list of factors does not take into account certain parameters of the ATLAS code. These parameters are:

- Known as having very little effect upon the particle's mechanical behaviour: the initial pressure of the gases found within the particle, the fuel grain size;
- Always associated with another parameter already subject to an uncertainty: porosity at the instant *t* (via the initial porosity);
- Not occurring in the mechanical model: the value of the anisotropy coefficient[9], the initial porosity of the kernel and SiC, the stoichiometry, density;

These parameters are set at their standard value.

| | DESCRIPTION | UNIT |
|---|---|---|
| TFAB | Manufacture temperature | K |
| KERNRAD | Initial kernel radius | m |
| BUFFTHIC | Initial buffer thickness | m |
| BUFFPORI | Initial buffer porosity | / |
| BUFFOPR | Initial buffer open porosity rate | / |
| IPYCTHIC | Initial thickness of the inner PyC layer | m |
| IPYCPORI | Initial porosity of the inner PyC layer | / |
| SICTHIC | Initial thickness of the SiC layer | m |
| OPYCTHIC | Initial thickness of the outer PyC layer | m |
| OPYCPORI | Initial porosity of the outer PyC layer | / |

TABLE 4 : PART FACTORS USED TO MODEL UNCERTAINTY ON THE PARTICLE MANUFACTURING PARAMETERS

| VARIABLE | DESCRIPTION | UNIT |
|---|---|---|
| PRESS | Pressure (constant) applied to the outer layer of the particle | Pa |
| ACC | Acceleration factor | n.m-2 |
| PFN | Nominal fission rate | s-1 |
| TIRR | Irradiation temperature | K |

TABLE 5 : REAC FACTORS USED TO MODEL UNCERTAINTY ON THE IRRADIATION CONDITIONS

[9] BAF: Bacon anisotropy factor. This coefficient is not taken into account by BNFL laws.

| | DESCRIPTION | UNIT |
|---|---|---|
| KERNNU | kernel Poisson's ratio | / |
| KERNYOUN | kernel Young's modulus | Pa |
| KERNDENS | kernel shrinkage | / |
| KERNGONG | kernel gas swelling | / |
| KERNGONS | kernel solid swelling | / |
| KERNGARR | fission gases release rate | / |
| KERNOPF | number of CO molecule created per fission | / |
| KERNLAMB | kernel thermal conductivity | W.m-1.K-1 |
| KERNALPH | kernel thermal expansion | K-1 |
| BUFFNU | buffer Poisson's ratio | / |
| BUFFYOUN | buffer Young's modulus | Pa |
| BUFFKFLU | buffer creep parameter | Pa-1.n-1.m2 |
| BUFFDENS | buffer shrinkage | / |
| BUFFLAMB | buffer thermal conductivity | W.m-1.K-1 |
| BUFFALPH | buffer thermal expansion | K-1 |
| PYCNU | PyC layers Poisson's ratio | / |
| PYCYOUN | PyC layers Young's modulus | Pa |
| PYCKFLU | PyC layers creep parameter | Pa-1.n-1.m2 |
| PYCDENR | PyC layers radial shrinkage | / |
| PYCDENT | PyC layers tangential shrinkage | / |
| PYCLAMB | PyC layers thermal conductivity | W.m-1.K-1 |
| PYCALPH | PyC layers thermal expansion | K-1 |
| SICNU | SiC layer Poisson's ratio | / |
| SICYOUN | SiC layer Young's modulus | Pa |
| SICKFLU | SiC layer creep parameter | Pa-1.n-1.m2 |
| SICDENS | SiC layer shrinkage | / |
| SICLAMB | SiC layer thermal conductivity | W.m-1K-1 |
| SICALPH | SiC layer thermal expansion | K-1 |

TABLE 6 : LAWS FACTORS USED TO MODEL UNCERTAINTY ON THE BEHAVIOUR LAWS

It is now necessary to define a probability distribution for each factor corresponding to the possible variations of this factor. Very little data is available on factor variations. Generally speaking, such data is sufficient to determine a minimum and maximum, which makes it possible to establish a uniform distribution. In certain cases, more data will make it possible to consider normal distributions. In absence of information, expert judgements will be used to establish reasonable hypotheses.

**Manufacturing parameters**

The uncertainties on the manufacturing parameters were determined as follows:

- *Layer thicknesses*: The document [13] provides measurement results for a particle sample; this document reveals the normality of the layer thicknesses; it was therefore decided to model these factors based on normal distributions; these distributions were truncated to avoid producing extreme results; manufacturing specifications recalled in [14] provide the average, minimum and maximum values; the standard deviation is lacking, which is determined via the coefficient of variation[10] that was set at 5% for all layers except the buffer which was set at 10%; these additional hypotheses are coherent with the document data [13];
- *Buffer and pyrolitic carbon porosities*: The specifications of the document [14] concern density; these data were converted in terms of porosity[11]; specifications do not state the maximum value of the buffer porosity, which we decided to set at 60%; furthermore, seeing that data on the open porosity rate of the buffer is unavailable, we decided to vary it between 80% and 100%;
- *Manufacturing temperature*: It was decided to vary this temperature between 1300 K and 1600 K;

The distributions of the particle manufacturing parameters are specified in Table 7.

| FACTORS | DISTRIBUTION |
|---|---|
| KERNRAD (μm) | Normal : min=230, max=270, mean=250, sd=12.5 (cv=5%) |
| BUFFTHIC (μm) | Normal : min=75, max=115, mean=95, sd=9.2 (cv=10%) |
| IPYCTHIC (μm) | Normal : min=30, max=50, mean=40, sd=2 (cv=5%) |
| SICTHIC (μm) | Normal : min=30, max=44, mean=35, sd=1.85 (cv=5%) |
| OPYCTHIC (μm) | Normal : min=30, max=50, mean=40, sd=2 (cv=5%) |
| TFAB (K) | Uniform : min=1300, max=1600 |
| BUFFPORI (%) | Uniform : min=50, max=60 |
| BUFFOPR (%) | Uniform : min=80, max=100 |
| IPYCPORI (%) | Uniform : min=11, max=18 |
| OPYCPORI (%) | Uniform : min=11, max=18 |

TABLE 7 : PROBABILITY DISTRIBUTIONS FOR PART FACTORS

**Irradiation parameters**

Data on the irradiation parameters are provided in Table 2. Determining the laws of variation based on these data was problematic for several reasons:

[10] The coefficient of variation (c.v. = standard deviation/ mean) is the standard deviation expressed as a percent of the mean. This is an indicator of the variation independent of the physical units.
[11] Porosity = $1 - \rho/\rho_{theoretical}$ with $\rho_{PyC} = 2.19$

- The pressure of interest is the pressure on the particle's outer surface; the pressure on the fuel element is known; in absence of specific information on the repercussion of this pressure upon the particles[12], it was decided to use 1 bar as the minimum for the HFR-EU2 (the maximum was set at 5 bar) and 60 bar for the GT-MHR (the maximum was set at 70 bar);
- No information on the fission rate variations (this quantity is also used in the PFN factor) is available; rather than this quantity, the irradiation time – specified in Table 2 – was directly varied; more specifically, if *T* represents the nominal irradiation time, it is varied in the interval [1/2, 3/2]**T*; the PFN factor therefore varies in the interval [2/3, 2] $*PFN_{nominal}$;
- The acceleration factor ACC characterises the reactor and can be varied very little; in the absence of information, this acceleration factor was attributed an uncertainty of 20% (±10%).

The distributions of the irradiation parameters are specified in Table 8.

| | | | GT-MHR | |
|---|---|---|---|---|
| | NOMINAL VALUE | UNIFORM DISTRIBUTION | NOMINAL VALUE | UNIFORM DISTRIBUTION |
| PRESS (bar) | 5 | min=1, max=5 | 70 | min=60, max=70 |
| ACC (1e26.n.m-2) | 4.48 | min=4.05, max=4.96 | 2.56 | min=2.30, max=2.81 |
| PFN (1e-9.s-1) | 3.3 | min=2.20, max=6.61 | 3.23 | min=2.15, max=6.47 |
| TIRR (K) | 1373 | min=1323, max=1423 | 975 | min=775, max=1175 |

TABLE 8 : PROBABILITY DISTRIBUTIONS FOR REAC FACTORS

**Behaviour laws**

Uncertainty on the laws describing the properties of materials is difficult to determine. Certain laws are deemed more reliable than others. It was decided to fix the same uncertainty on all laws to enable comparison between them. Uncertainty is set at 10% (±5%) and introduced in the following manner: the behaviour laws are multiplied by a factor that varies according to a uniform distribution on [0,95; 1,05].

Now that we have established the list of factors with their probability laws and responses to be investigated, it is possible to begin the sensitivity studies.

[12] The pressure field in a fuel compact will need to be calculated to do this.

# 4. HFR-EU2 REACTOR CONFIGURATION STUDY

Our first study falls within the scope of the test reactor HFR-EU2.

## 4.1. EFFECT OF MANUFACTURING PARAMETERS

To study the influence of particle manufacturing parameters, the first set of factors was varied according to the laws defined in Table 7. The factors corresponding to the irradiation parameters (REAC factors) were set at their constant nominal value (cf. Table 8). The behaviour laws also retained their normal values; the LAWS factors were constant and equal to 1. This study only took into account uncertainty related to particle manufacturing.

**Uncertainty analysis**

A sample[13] of 500 values was generated. The code was operated on this sample, which represented 14 hours of computation. Three responses were then obtained from the results for the 500 simulations, which resulted in a 500-sample for each response.

The histogram corresponding to the sample of the second response is represented in Figure 7 (stress in the SiC layer). It is clear that this response follows a normal distribution[14]. The two other responses also followed normal distributions (they are not represented).

The elementary statistics corresponding to the laws of the three responses are illustrated in Figure 7. It was remarked that the coefficient of variation was rather small for the PyC layers (less than 2%) and much bigger for the SiC layer (30%). Uncertainty on stress is therefore located in the SiC layer.

**Influence analysis**

It has just been seen that only stress in the SiC layer is subject to uncertainty. We shall now try to explain this uncertainty by analysing influences, with the aim of determining the factors responsible for this uncertainty.

[13] This was an LHS-type sample, cf. [SCS 00].
[14] In all our studies, normality was confirmed by KOLMOGOROV-SMIRNOV tests. The statistical figures are not specified but this point was correctly verified.

Based on the sample used to perform the uncertainty analysis, the model linear regression was completed, proving to be of very good quality ($R^2 = 0.98$). This regression made it possible to calculate the PEAR and SRC indices discussed in subsection 2.2. It must be recalled that the SRC indices quantify influence in terms of a percent of the factor. Regarding the PEAR indices, their sign is used to interpret the direction of the influence. The indices estimated for the sample are represented in Figure 8.

The SRC indices revealed that only three factors were responsible for more than 90% of the stress variance: the kernel radius and buffer thickness (about 40% each), and the buffer porosity (more than 10%).

The PEAR indices indicate in which direction these factors influence. Therefore:

- Stress increases when the kernel radius increases; a bigger kernel represents more fuel and therefore more released gases;
- Stress decreases when the buffer thickness increases: a bigger buffer represents more available space for the released gases;
- Stress decreases when the buffer porosity increases: the reason above also applies here.

The three factors responsible for stress variations in the SiC layer are therefore related to the release of gases. It is therefore reasonable to believe that this phenomenon alone is behind the significant stress variations in the SiC layer.

## 4.2. BEHAVIOUR UNDER IRRADIATION

The influence of the particle manufacturing parameters has now been characterised with constant irradiation conditions. This is not realistic on the scale of the particle population in the reactor core. The two first sets of factors were therefore varied (PART and REAC); the behaviour laws (LAWS factors) remained undisturbed.
From now on, all our studies will follow the same approach as the one that has just been applied. This approach will no longer be detailed; only the results will be given.

**Uncertainty analysis**

The results (cf. Figure 9) are similar to those obtained in the previous study: only the stress in the SiC layer varies, with these variations following a normal distribution. Therefore, the influence analysis was performed for the SiC layer only.

**Influence analysis**

The linear regression proved to be very good again; the PEAR and SRC index methods were thus applied. These indices are represented in Figure 10. Only four factors are responsible for more than 70% of the stress variations: the kernel radius (26%), the buffer thickness (24%), the irradiation temperature (13%) and the acceleration factor (11%). The order of influence of the particle manufacturing factors is comparable to that of the previous study. The influence of the irradiation conditions is considerable (25%) and is conditioned by both the irradiation temperature and the acceleration factor. This result is qualified because the data on these two parameters is inadequate. It can only be said that these two parameters are potentially influential and a better understanding of the range of these parameters would make it possible to refine this result.

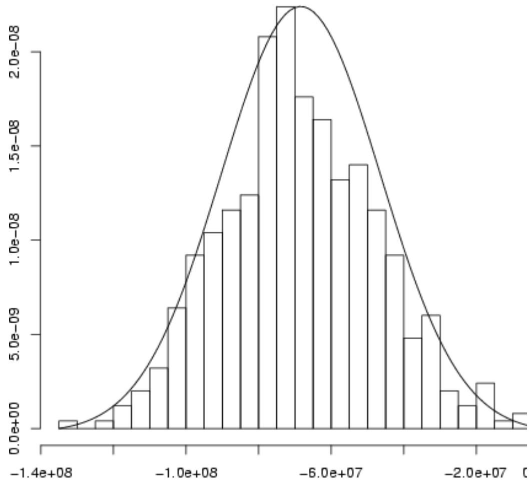


Histogram of maximum tangential stress in SiC layer

| Statistics | maximum tangential stress | | |
|---|---|---|---|
| | IPyC | SiC | OPyC |
| Min. (MPa) | 171 | -133 | 101 |
| moy. (MPa) | 184 | -68 | 103 |
| max. (MPa) | 198 | -8 | 104 |
| coef. var. (%) | 2 | **30** | <1 |

FIGURE 7 : HFR-EU2 – UNCERTAINTY ANALYSIS RELATED TO MANUFACTURING PARAMETERS

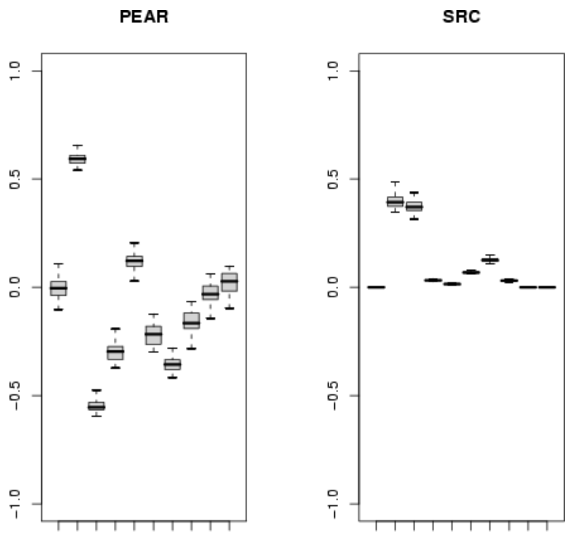


| Factor | PEAR | SRC |
|---|---|---|
| TFAB | -0.01 | 0.0 |
| KERNRAD | 0.59 | **0.40** |
| BUFFTHIC | -0.55 | **0.37** |
| IPYCTHIC | -0.29 | 0.03 |
| SICTHIC | 0.13 | 0.02 |
| OPYCTHIC | -0.23 | 0.07 |
| BUFFPORI | -0.34 | **0.13** |
| BUFFOPR | -0.16 | 0.03 |
| IPYCPORI | -0.03 | 0.0 |
| OPYCPORI | 0.02 | 0.0 |

Estimations of PEAR and SRC indices for maximum tangential stress in SiC Layer

FIGURE 8 : HFR-EU2 – INFLUENCE ANALYSIS OF THE MANUFACTURING PARAMETERS

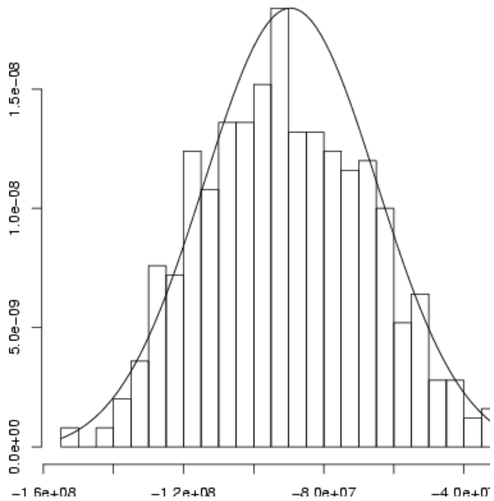


| statistics | maximum tangential stress | | |
|---|---|---|---|
| | IPyC | SiC | OPyC |
| min. (MPa) | 172 | -154 | 101 |
| moy. (MPa) | 184 | -90 | 103 |
| max. (MPa) | 196 | -16 | 106 |
| coef.var. (%) | 2 | **26** | <1 |

Histogram of maximum tangential stress in SiC layer

FIGURE 9 : HFR-EU2 – UNCERTAINTY ANALYSIS RELATED TO THE MANUFACTURING AND IRRADIATION PARAMETERS

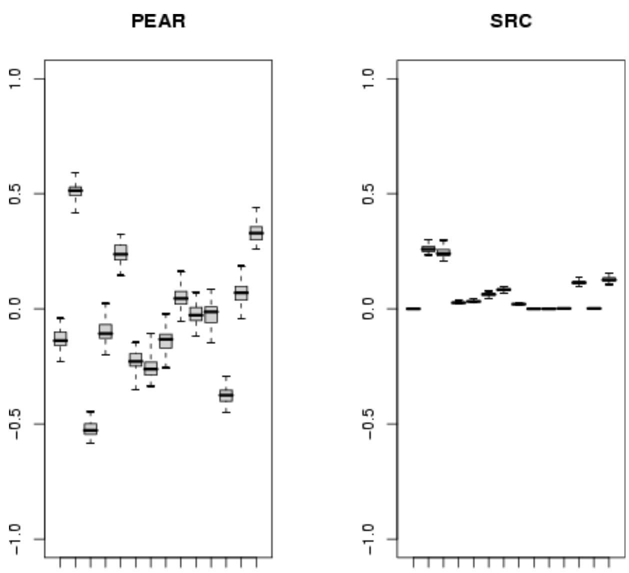


| Factor | PEAR | SRC |
|---|---|---|
| TFAB | -0.13 | 0.0 |
| KERNRAD | 0.51 | **0.26** |
| BUFFTHIC | -0.52 | **0.24** |
| IPYCTHIC | -0.1 | 0.03 |
| SICTHIC | 0.24 | 0.03 |
| OPYCTHIC | -0.23 | 0.06 |
| BUFFPORI | -0.26 | 0.08 |
| BUFFOPR | -0.14 | 0.02 |
| IPYCPORI | 0.05 | 0.0 |
| OPYCPORI | -0.02 | 0.0 |
| PRESS | -0.02 | 0.0 |
| ACC | -0.38 | **0.11** |
| PFN | 0.07 | 0.0 |
| TIRR | 0.33 | **0.13** |

Estimations of PEAR and SRC indices for maximum tangential stress in SiC Layer

FIGURE 10 : HFR-EU2 – INFLUENCE ANALYSIS OF THE MANUFACTURING AND IRRADIATIONPARAMETERS

# 5. GT-MHR REACTOR CONFIGURATION STUDY

The same studies as those performed for the HFR-EU2 will now be carried out for the GT-MHR. The first two studies will follow exactly the same approach as specified for the studies discussed in subsections 4.1 and 4.2. The approach will no longer be detailed. Furthermore, a sensitivity analysis will be performed taking into account uncertainty related to behaviour laws.

## 5.1. EFFECT OF MANUFACTURING PARAMETERS

It is to be remembered that only the PART factors are varied in this study.

**Uncertainty analysis**

The stress distributions are shown in Figure 11. The stress in the PyC layers varies very little (c.v. < 3%). The stress in the SiC layer displays a coefficient of variation of 11% and follows a normal distribution. Uncertainties on the particle manufacturing parameters therefore affect the stress in the SiC layer. The variations are smaller than in the case of the HFR-EU2.

**Influence analysis**

The influence was analysed for the second stress so as to explain the uncertainty that we just revealed. The linear regression performed on the sample used to analyse uncertainty was of high quality. The PEAR and SRC index method was applied once again, which is represented in Figure 12. It was observed that the layer thicknesses represented 96% of the influence. By increasing order of influence, the following results were obtained: the buffer thickness (29%), SiC layer thickness (27%), the kernel radius (16%) and the outer and inner PyC layer thicknesses (13% and 11% respectively).

It is worth pointing out the importance of the SiC layer thickness. This phenomenon was not observed in the HFR-EU2. This point will be studied in detail in section 6.

## 5.2. BEHAVIOUR UNDER IRRADIATION

It is to be remembered that this study involves varying both PART and REAC factors.

**Uncertainty analysis**

The results (cf. Figure 13) are similar to those obtained in the previous study: only the stress in the SiC layer varies, with these variations following a normal distribution. Analysis of the influence is therefore only carried out for the SiC layer.

**Influence analysis**

The linear regression also proved to be of high quality, with the PEAR and SRC index method being used once again. These indices are represented in Figure 14. Only four factors are responsible for more than 65% of the stress variation: the irradiation temperature (29%), buffer thickness (17%), SiC layer thickness (14%) and the kernel radius (12%). The manufacturing parameters are decisive as a whole (72% influence). Nevertheless, the irradiation temperature proves to be the most influential (30%).
In comparison to the HFR-EU2 study, the SiC layer thickness becomes influential (as previously observed). However, the acceleration factor no longer proves to be influential. This last point can be partially explained by the fact that this factor varies proportionally and is two times less significant in the HFR-EU2, which means that its variations are two times less significant.

## 5.3. SENSITIVITY TO BEHAVIOUR LAWS

This study aims at evaluating the model sensitivity to variations in behaviour laws. It must be remembered that the behaviour laws (LAWS factors) are disrupted by ±5% in a uniform manner. The factors of the two other groups were also varied (PART and REAC). The behaviour laws must be qualified while taking into account all acceptable values for the other parameters.

**Uncertainty analysis**

The uncertainty analysis was performed in the same manner based on a group of 500 samples. The results are illustrated in Figure 15. The stress variations in the PyC layers increased slightly (up to 4%). These variations were still too small to conduct a sensitivity analysis. The stress variations in the SiC layer did not change in comparison to the previous study, remaining considerable (c.v. = 11%).

Only stress variations in the PyC layers increased. It can therefore be thought that the influential models involve these layers. The sensitivity analysis will make it possible to confirm if the PyC layer models do indeed affect the stress in the SiC layer.

**Sensitivity analysis**

It was decided to study sensitivity rather than influence. The uncertainty attributed to the behaviour laws (±5%) was arbitrary in comparison to uncertainty on the other factors. An influence analysis should take into account this uncertainty in a comprehensive manner. On the contrary, a sensitivity analysis makes it possible to measure the impact of small factor variations upon the response (these local variations are taken into account over the whole variation range of the laws [-5%, +5%]. Therefore, a sensitivity analysis makes it possible to know if a law has the potential of influencing the response. This influence will be effective if uncertainty on the law is considerable.

We chose to use the MORRIS method discussed in section 2.2. This method is used to classify the factors by increasing sensitivity and requires very few simulations for a large number of factors, which makes it perfectly suitable for our situation (42 factors).

A sample group of 860 values was generated to form a MORRIS OAT experiment design (5 levels, 20 repetitions). Based on the simulation results established with this experiment design, the statistics $\mu^*$ and $\sigma$ were estimated. The results are provided in Figure 16. The $\mu^*$ axis represents the degree of sensitivity. The following was observed:

- Stress in the SiC layer was mainly sensitive to the geometric parameters (layer thicknesses) and the irradiation temperature; a high sensitivity to variations in the thickness of the outer layers was observed (IPYCTHIC, SICTHIC, OPYCTHIC); these variations were low, which explains why no influence from these three parameters was detected in the previous studies;
- In terms of behaviour laws, the PyC creep coefficient (PYCKFLU) and PyC tangential densification (PYCDENT) proved to be the only parameters to which stress was sensitive; it remains to be known if these behaviour laws are well-known or not.

The $\sigma$ axis represents the non-linear effects and interactions. These values are low, which indicates that the factors have more or less linear effects with low interaction. This had already been revealed in previous influence studies where linear regression was validated. The behaviour laws therefore do not contribute any non-linearities.

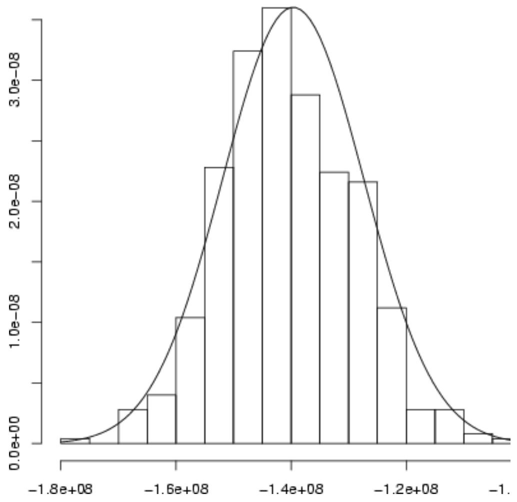


Histogram of maximum tangential stress in SiC layer

| statistics | maximum tangential stress | | |
|---|---|---|---|
| | IPyC | SiC | OPyC |
| min. (MPa) | 172 | -179 | 94 |
| moy. (MPa) | 185 | -140 | 97 |
| max. (MPa) | 202 | -97 | 100 |
| coef. var. (%) | 2.4 | **8** | <1 |

FIGURE 11 : GT-MHR – UNCERTAINTY ANALYSIS RELATED TO THE MANUFACTURING PARAMETERS

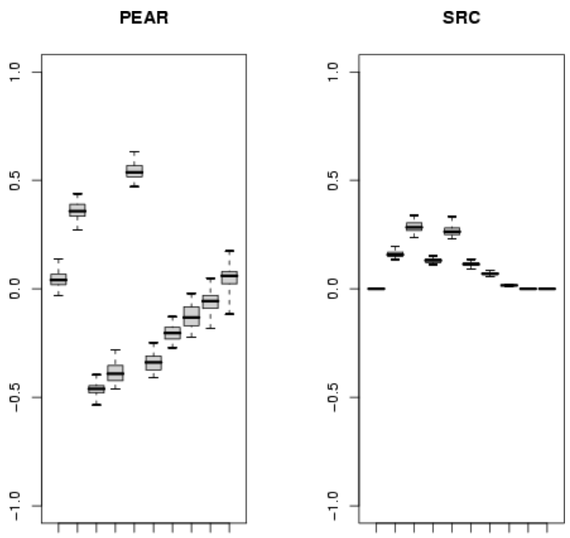


| Factor | PEAR | SRC |
|---|---|---|
| TFAB | 0.05 | 0.0 |
| KERNRAD | 0.36 | **0.16** |
| BUFFTHIC | -0.46 | **0.29** |
| IPYCTHIC | -0.39 | **0.13** |
| SICTHIC | 0.54 | **0.27** |
| OPYCTHIC | -0.34 | **0.11** |
| BUFFPORI | -0.2 | 0.07 |
| BUFFOPR | -0.13 | 0.02 |
| IPYCPORI | -0.06 | 0.0 |
| OPYCPORI | 0.05 | 0.0 |

Estimations of PEAR and SRC indices for maximum tangential stress in SiC Layer

FIGURE 12 : GT-MHR – INFLUENCE ANALYSIS OF THE MANUFACTURING PARAMETERS

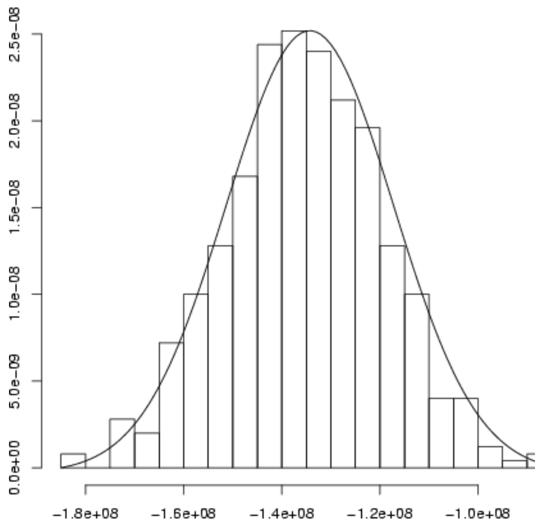


| statistics | maximum tangential stress | | |
|---|---|---|---|
| | IPyC | SiC | OPy C |
| min. (Mpa) | 171 | -183 | 95 |
| moy. (Mpa) | 184 | -135 | 97 |
| max. (MPa) | 197 | -89 | 100 |
| coef.var. (%) | 2 | **11** | <1 |

Histogram of maximum tangential stress in SiC layer

FIGURE 13 : GT-MHR – UNCERTAINTY ANALYSIS RELATED TO THE MANUFACTURING AND IRRADIATION PARAMETERS

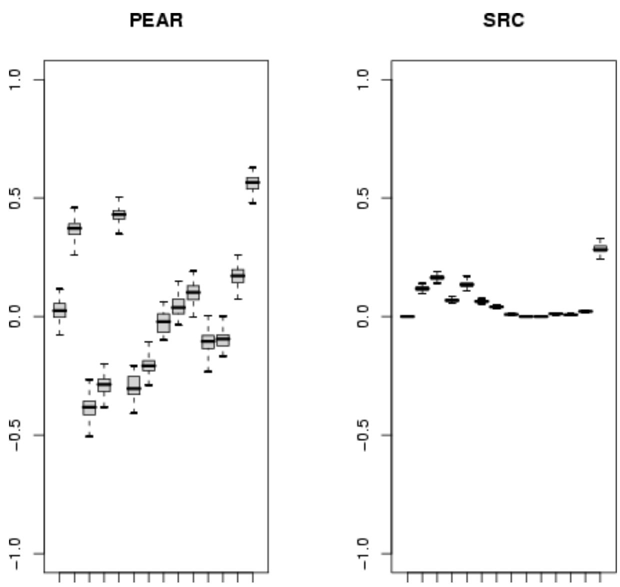


| Factor | PEAR | SRC |
|---|---|---|
| TFAB | 0.02 | 0.0 |
| KERNRAD | 0.37 | **0.12** |
| BUFFTHIC | -0.39 | **0.17** |
| IPYCTHIC | -0.29 | 0.07 |
| SICTHIC | 0.43 | **0.14** |
| OPYCTHIC | -0.3 | 0.06 |
| BUFFPORI | -0.21 | 0.04 |
| BUFFOPR | -0.02 | 0.01 |
| IPYCPORI | 0.04 | 0.0 |
| OPYCPORI | 0.1 | 0.0 |
| PRESS | -0.11 | 0.01 |
| ACC | -0.09 | 0.01 |
| PFN | 0.17 | 0.02 |
| TIRR | 0.56 | **0.29** |

Estimations of PEAR and SRC indices for maximum tangential stress in SiC Layer

FIGURE 14 : GT-MHR – INFLUENCE ANALYSIS FOR THE MANUFACTURING AND IRRADIATION PARAMETERS

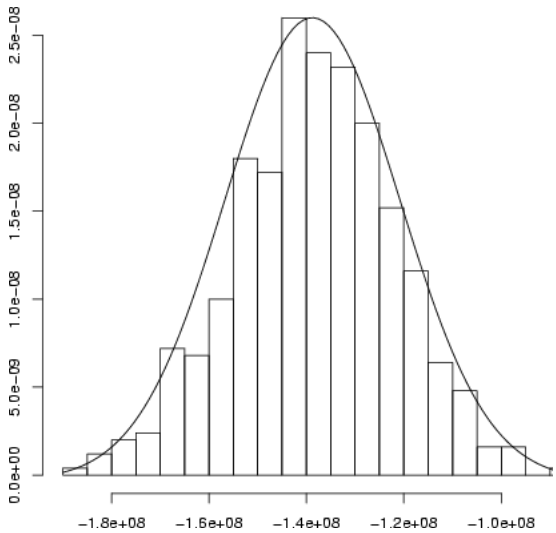


Histogram of maximum tangential stress in SiC layer

| statistics | maximum tangential stress | | |
|---|---|---|---|
| | IPyC | SiC | OPyC |
| min. (MPa) | 165 | -185 | 88 |
| moy. (MPa) | 184 | -138 | 97 |
| max. (MPa) | 208 | -89 | 107 |
| coef. var. (%) | 4 | **11** | 4 |

FIGURE 15 : GT-MHR – UNCERTAINTY ANALYSIS RELATED TO THE MANUFACTURING AND IRRADIATION PARAMETERS AND THE BEHAVIOUR LAWS

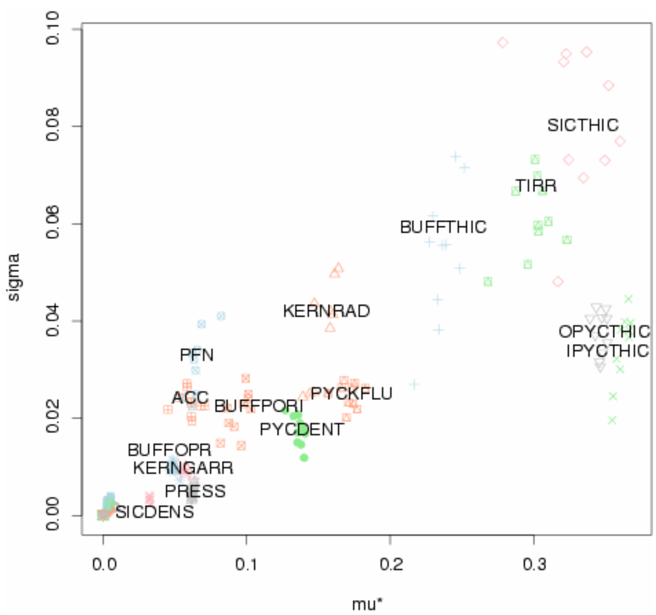


The MORRIS sensitivity measurement estimates are represented by the graph (μ*, σ). μ* represents the sensitivity whereas σ represents the interactions or non-linear effects. The symbols surrounding the factor names represent the bootstrap replicas, which makes it possible to visually observe the high quality of the estimates.

FIGURE 16 : GT-MHR – SENSITIVITY ANALYSIS FOR THE MANUFACTURING AND IRRADIATION PARAMETERS AND THE BEHAVIOUR LAWS

# 6. EFFECT OF IRRADIATION TEMPERATURE

The results of studies on the influence of particle manufacturing parameters for the HFR-EU2 (subsection 4.1) and the GT-MHR (subsection 5.1) configurations were compared. In terms of the HFR-EU2 configuration, the buffer thickness proved to be highly influential (37%) whereas the SiC layer showed to have very little influence at all (2%). For the GT-MHR, the buffer thickness was clearly less influential (29%) and whereas the SiC layer proved to be much more influential (27%).

This difference is due to the irradiation conditions. The irradiation parameters and the particle manufacturing parameters therefore interact. The MORRIS method shows (cf. Figure 16) that the irradiation parameter most likely to be involved in interactions is the irradiation temperature (the irradiation temperature TIRR is observed to have the greatest $\sigma$ value) for the GT-MHR configuration. The following hypothesis was therefore reached: the irradiation temperature is responsible for the difference in behaviour observed between the HFR-EU2 and GT-MHR configurations.

In order to verify this hypothesis, several simulations were performed, during which the irradiation temperature, buffer thickness and SiC layer thickness were varied. In terms of the other parameters, the nominal values were taken into account, placed under HFR-EU2 conditions.

**High irradiation temperature**

For this first experiment, the irradiation temperature was set at 1423 K, which is the maximum temperature in our studies (this temperature is reached in the HFR-EU2). Four simulations were performed:

- Two simulations varying the buffer thickness between its minimum and maximum; the SiC layer thickness was set at a mean value;
- Two simulations varying the SiC layer thickness between its minimum and maximum; the buffer thickness was set at a mean value.

The results are shown in Figure 17. It was observed that the buffer thickness has a greater influence upon the final stress value than the SiC layer thickness.

**Low irradiation temperature**

For this second experiment, the irradiation temperature was set at 775 K, which represents the minimum temperature in our studies (this temperature is reached in the GT-MHR). Four simulations were performed, as was the case in the first experiment. The results are illustrated in Figure 18. It was observed that the buffer thickness has less effect than the SiC layer thickness. It is also worth pointing out that the stress is lower at low temperature than it is at high temperature.

**Conclusion**

Strong interaction between the irradiation temperature and certain particle manufacturing parameters has been demonstrated. This interaction is responsible for a behaviour change. At high temperature, the buffer thickness has more effect upon the final stress value than that of the SiC layer. At low temperature, the SiC layer thickness has more effect upon the final stress value than the buffer thickness. The SiC layer thickness tends to vary very little in comparison to the buffer thickness (±7 µm for SiC and ±20 µm for the buffer). The high influence of the SiC layer for such low variations therefore points to a very high sensitivity.

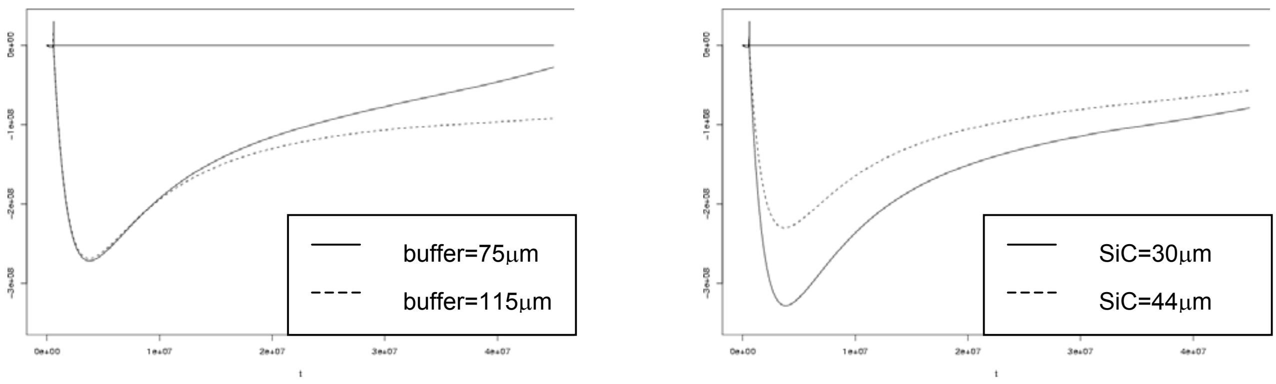


FIGURE 17 : INFLUENCE OF THE IRRADIATION TEMPERATURE (1423 K)

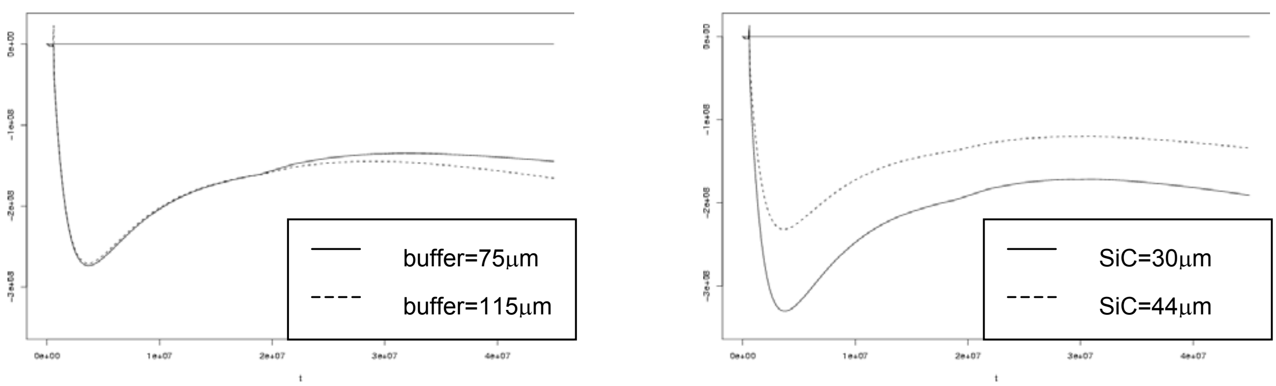


FIGURE 18 : INFLUENCE OF THE IRRADIATION TEMPERATURE (775 K)

# 7. CONCLUSION

This study aims at characterising the behaviour of the ATLAS computational code by taking into account the impact of different uncertainties on input parameters. Here is a review of the different issues discussed in this report:

**Bibliography**

The reasons for applying a sensitivity analysis approach are clearly specified: uncertainty is necessarily associated with the results when using a computational code. Different analytical methods are described. A distinction is made between qualitative and quantitative methods:

- MORRIS method is used to characterise the sensitivity of the model to variations in the different parameters; this method only requires a low number of simulations and is effective even in the presence of many parameters;
- Methods based on variance decompositions (SRC indices, SOBOL method and FAST method) making it possible to estimate the influence as a percentage of each parameter; these methods are rather complex, except in the case of a linear regression.

Thus, this theoretical investigation has enabled us to develop tools designed to perform sensitivity analyses on any computational code.

**ATLAS code sensitivity studies**

First of all, three sources of uncertainty are revealed:

1. Uncertainty on particle manufacturing parameters;
2. Uncertainty on irradiation conditions;
3. Uncertainty on behaviour laws.

Then, the consequences of such uncertainties upon stress in the outer layers (IPyC, SiC, OPyC) are investigated.

The uncertainty analysis shows that only stress in the SiC layer is subject to considerable uncertainty. The stress in the PyC layers varies very little.

The influence and sensitivity analyses conducted on the stress in the SiC layer provide the following results:

- The particle manufacturing parameters are always very influential, particularly the kernel radius, buffer thickness and buffer porosity;

- The influence of the irradiation conditions are only felt through the irradiation temperature; this parameter interacts with the particle manufacturing parameters; the real influence of the acceleration factor[15] is uncertain owing to the lack of specific data on this quantity;
- The model only proved to be sensitive to the following behaviour laws : creep and tangential shrinkage of PyC.

**Conclusion and future prospects**

This preliminary statistical study on the ATLAS code demonstrates the high capacity of sensitivity analysis methods. By studying the ATLAS code results for a large number of simulations, it has been possible to acquire a better understanding of the behaviour of this computational code and even more so of the fuel particles. These preliminary results leave us with the following possibilities:

- The influential parameters have been identified; it is now question of improving our knowledge of these parameters; therefore, reducing uncertainty related to such parameters will help reduce the most significant uncertainty on stress; more particularly, enhanced modelling of irradiation parameter uncertainty would make it possible to significantly refine results;
- A direct application of our research involves determining the broadest range of particle manufacturing specifications while remaining below a given particle failure rate; to do this, the variation range of the least influential parameters needs to be gradually increased;
- The sensitivity analyses could be continued using a 2D geometry; it would therefore be possible to take into account parameters that are known to be influential and that do not intervene in 1D geometry; this is, for example, the case of sphericity defects.

[15] Acceleration factor = neutron flux/ fission rate

# REFERENCES

1 A. SALTELLI, K. CHAN & E.M. SCOTT. Sensitivity Analysis. Series in Probability and Statistics. Wiley, 2000.

2 PHILIPPE BESSE. *Pratique de la modélisation statistique*. Publication of Laboratoire de Statistique et Probabilités, Université Paul Sabatier, 2003.

3 J. JACQUES. *Contribution à l'analyse de sensibilité et à l'analyse discriminante généralisée*. PhD Thesis : Université Joseph Fourier - Grenoble 1, 2005.

4 A SALTELLI, S. TARANTOLA & K. CHAN. A quantitative model-independent method for global sensitivity analysis of model output. Technometrics. Vol. 41, pp. 39–56, 1999.

5 F. MICHEL. *Notice d'utilisation d'ATLAS V1.0*. Technical report, CEA/DEN/CAD/DEC/SESC/LSC, 2003.

6 M. LAINET. *Presentation of ATLAS V2.0*. Technical report, CEA/DEN/CAD/DEC/SESC/LSC, 2005.

7 M. FÜTTERER, H. LOHNER, A. MARNIER, S. DE GROOT & C. SCIOLLA. Preliminary results from an avr fuel pebble irradiation at increased temperature and burn-up in the hfr petten. *International congress on advances in nuclear power plants*. 2005. paper 5296.

8 A. LANGUILLE. *HTR coated particles and fuel elements - present development*, 2002. High temperature reactor school.

9 M. LABAR, W. SIMON, A. SHENOY & T. QUINN. Design status of the gas turbine – modular helium reactor : An advanced nuclear power system for near term deployment. *Americas Nuclear Energy Symposium*. 2002.

10 P. CHAPELOT, A. LANGUILLE, X. RAEPSAET & D. HITTNER. Requirements for high temperature reactor fuel particle design assessment. *Progress in Nuclear Energy*. Vol. 38, pp. 415–418, 2001.

11 *Fabrication du combustible HTR*, 2001. Minutes of meeting, May 3 2005, Cadarache, CR LCU01-010.

12 G. K. MILLER, D. A. PETTI, D. J. VARACALLE & J. T. MAKI. Statistical approach and benchmarking for modeling of multi-dimensional behaviour in TRISO-coated fuel particles. *Journal of Nuclear Materials*. Vol. 317, pp. 69–82, 2003.

13 J.D. HUNN. *Results from ONRL characterization of german reference fuel from EUO 2358-2365 composite*. Technical report, OAK Ridge National Laboratory, 2004.

14 M. PHELIP. European programme on high and very high temperature reactor fuel technology. International congress on advances in nuclear power plants. 2005. paper 5160.

# LIST OF TABLES

# LIST OF FIGURES